RADIO AND OPTICAL INVESTIGATIONS OF MIDDLE AND UPPER ATMOSPHERE OVER INDIA

G. K. MUKHERJEE[1] AND S. GURUBARAN[2]

The Indian peninsular region has a unique geographical identity – the tropical convection is intense here resulting in a spectrum of convectively generated gravity waves. The latitudinal variation of the Coriolis frequency is such that certain long-period (of a few days) eastward propagating waves are trapped in the middle atmospheric region over these low latitudes. The short-period gravity waves carry significant energy and momentum flux and are able to propagate to great heights into the upper atmosphere. The ionized layers in the upper atmospheric region are influenced by the configuration of the geomagnetic field which becomes nearly horizontal as the tip of the Indian peninsular region is reached. Intense current jet in the lower E region, the plasma fountain encompassing the low latitude E and F regions, the ionization irregularities in the F region contributing to the Spread-F phenomena are the prominent features of the equatorial ionosphere. Upward propagating tides and gravity waves are important sources of variability of both middle and upper atmosphere, whereas the ionosphere-magnetosphere interactions at high geomagnetic latitudes during magnetic disturbances produce certain noticeable effects on the equatorial upper atmosphere. The Indian middle and upper atmospheric science communities have their strengths in pursuing intense experimental studies with state-of-the-art facilities available at a number of locations. This paper reviews some of the recent advances made by the Indian atmospheric science community in the pursuit of understanding the spatial and temporal variabilities of some of the dynamical and electrodynamical phenomena occurring in the middle and upper atmosphere over the Indian sector using radio and optical techniques.

Introduction

The various regions of the Earth's middle and upper atmosphere constitute a closely coupled system driven by a variety of physical and chemical processes. It is widely accepted that there is continuous transfer of energy, mass and momentum between the atmospheric regions that were earlier demarcated by distinct boundaries or pauses. For example, wave processes of lower atmospheric origin characterized by upward energy and momentum transports clearly have some of their signatures in the ionized upper atmospheric regions[1]. There is a transport of atomic oxygen from the lower thermosphere, where photodissociation of molecular oxygen readily takes place, to the mesopause region where the oxygen atoms recombine and release the stored chemical energy[2]. The temporal variations in the F-region electrodynamics at low latitudes are now believed to be strongly controlled by the tides propagating from below[3,4].

Apart from the effects of wave perturbations of neutral atmospheric origin, the upper atmosphere in the equatorial region is influenced by disturbances of solar origin[5]. In particular, the interplanetary electric fields can promptly penetrate to the equatorial latitudes at certain times that show up in the stormtime ionospheric response. A disturbance of dynamo origin also propagates from high latitudes to equatorial latitudes during major magnetic storms. Space weather is an important issue in recent times as disturbances in the ionosphere can affect the satellite navigation and communication systems[6]. An understanding

1 Indian Institute of Geomagnetism, New Panvel, Navi Mumbai 410 218, e-mail:gkm@iigs.iigm.res.in

2 Equatorial Geophysical Research Laboratory, Indian Institute of Geomagnetism, Krishnapuram, Tirunelveli 627 011, e-mail: gurubara@iigs.iigm.res.in

of the evolution of ionospheric irregularities at low latitudes during magnetic storms is important for space weather monitoring and forecasting. Several observational tools are now available to assess the response of the equatorial ionosphere to disturbances resulting from solar wind-magnetosphere-ionosphere interactions.

The Indian scientific community has made significant progress during the last couple of decades in several of the above areas. Deployment of optical and radio probing instruments and UHF/VHF receivers at a large number of sites and well-planned balloon and rocket soundings had led to several coordinated studies performed through specific experimental campaigns addressing to middle atmosphere[7] and the ionosphere-thermosphere at low latitudes[8,9,10]. This paper reviews some of the results from such studies during the last decade and the progress made in our understanding of the dynamical and electrodynamical processes operative in the near space environment.

Middle Atmosphere

Long-period oscillation : There are two distinct middle atmospheric phenomena occurring in the tropics with time scales longer than that of a season: (a) quasi-biennial oscillation (QBO) and (b) semi-annual oscillation (SAO). The Indian scientific community had conducted active rocket and balloon sounding programmes in the past to quantify the middle atmospheric responses to the forcings responsible for these long-period oscillations[11,12]. During the last decade, a national programme called 'ISRO's Middle Atmosphere Dynamics Programme – MIDAS' was conducted during the period 2002-2005 that involved a number of RH200 rocket and high altitude balloon launches at Thumba accompanied by ground-based observations using radars at Trivandrum (8.5°N, 77°E), Tirunelveli (8.7°N, 77.8°E) and Gadanki (13.5°N, 79.2°E) and lidar at Gadanki[13]. One of the objectives of this programme has been to quantify the role of gravity waves in the evolution of the easterly and westerly phases of both stratopause and mesopause SAO.

The QBO is characterized by alternating easterly and westerly winds in the tropical stratosphere with a period of about 28 months[14]. The amplitude of the oscillation is about 20 ms^{-1} in the lower stratosphere, with a phase descent of approximately 1 km per month. The QBO has a latitude structure that has a characteristic decrease of amplitude to half its maximum at the equator by 15° latitude. It was initially proposed that the forcing of the QBO was provided by Kelvin and Rossby gravity waves propagating vertically from the troposphere[15]. Subsequent reports showed that additional momentum sources are required in order to obtain a realistic QBO in the model simulations and gravity waves are now believed to provide the additional forcing needed to drive the QBO[14]

A recent work made use of long-term Rayleigh lidar temperature observations made at Gadanki and quantified the role of gravity waves in driving the easterly and westerly phases of the QBO[16]. The mean flow acceleration computed from the monthly mean zonal winds derived from the NCEP/NCAR reanalysis data at 10 and 20 hPa was compared with the mean flow acceleration derived from the momentum fluxes estimated from the lidar temperature observations. This exercise reveals that the contribution of the gravity waves towards the westerly phase of the QBO is in the range 10-60% while that during easterly phase is in the range 10-30%.

The semi-annual oscillation is the other low frequency variability in the tropical middle atmosphere first recorded using rocket observations in the stratosphere[17]. It was shown later that the SAO consists of two oscillations with amplitude maxima near the stratopause and mesopause with minimum near 64 km with the two oscillations exhibiting out-of-phase behaviour[18]. As with the QBO, it was emphasized in recent years that the small-scale gravity waves play an important role in driving the SAO[19,20]. From ground-based lidar and rocket sounding observations obtained during the Equatorial Wave Studies (EWS) campaign[19], a mean flow acceleration of ~25 $ms^{-1}month^{-1}$ was computed that was representative of the gravity wave contribution near the stratopause whereas the rocketsonde derived mean flow acceleration at this height was ~40 $ms^{-1}month^{-1}$. A linear increase in the computed mean flow acceleration from 35 km onwards clearly delineates the role of gravity waves in driving the mean zonal flow in the upper stratosphere and lower mesosphere.

In the equatorial mesosphere-lower thermosphere (MLT) region (80-100 km), the mean zonal wind is characterized by a predominant semi-annual variability with westward winds during equinox and eastward winds during solstice[21]. It was first revealed by satellite observations that the first westward phase of the mean zonal wind undergoes interannual variability with large westward wind flow occurring during alternate years, and this variability has been interpreted as a signature of the QBO in the MLT region[22]. In particular, ground-based radar and satellite wind observations clearly indicate a stronger westward phase during spring equinoxes when deep QBO eastward winds are present in the middle stratosphere. Recently, long-term MF radar observations from Tirunelveli were used to examine the year-to-year variation in the amplitude of one of the two peaks of the SAO in zonal wind and compare its relation with the stratospheric QBO[23]. Fig. 1 depicts the long-term (1993-2006) mean zonal winds at MLT heights and the radiosonde derived QBO

winds in the height region 90-3 hPa. It can be noticed that large westward winds at MLT heights that are seasonally locked to spring equinox, occur only when there are strong eastward winds at all pressure levels in the stratosphere. The QBO was observed to be irregular between 1998 and 2001 when the period was nearly 3 years and correspondingly the maximum westward SAO phase was pushed to the third year. For large westward winds at MLT heights to occur, both stratospheric QBO and SAO are required to be in their eastward phases. These narrow regimes of eastward winds at all heights below the mesosphere are expected to provide favourable conditions for the westward propagating waves to carry westward momentum to the MLT region driving large westward winds there.

utilized the MF radar data sets from Tirunelveli focused on the short-term variability of tides, mean winds and gravity waves during the westward phase of the MSAO and proposed that the short-term tidal variability contributes, either directly, or indirectly through the gravity wave-tidal interactions, to the variation of the strength of the time-mean westward flow associated with the MSAO[26].

The other long-period oscillation that has been studied in the past is the intraseasonal oscillation (ISO) in the MLT region zonal wind[23,27,28]. These studies have shown that the equatorial waves that are capable of driving a Madden-Julian Oscillation (MJO) in the tropical lower atmosphere do not propagate directly into the MLT region, whereas it has been suggested that the ISO observed in

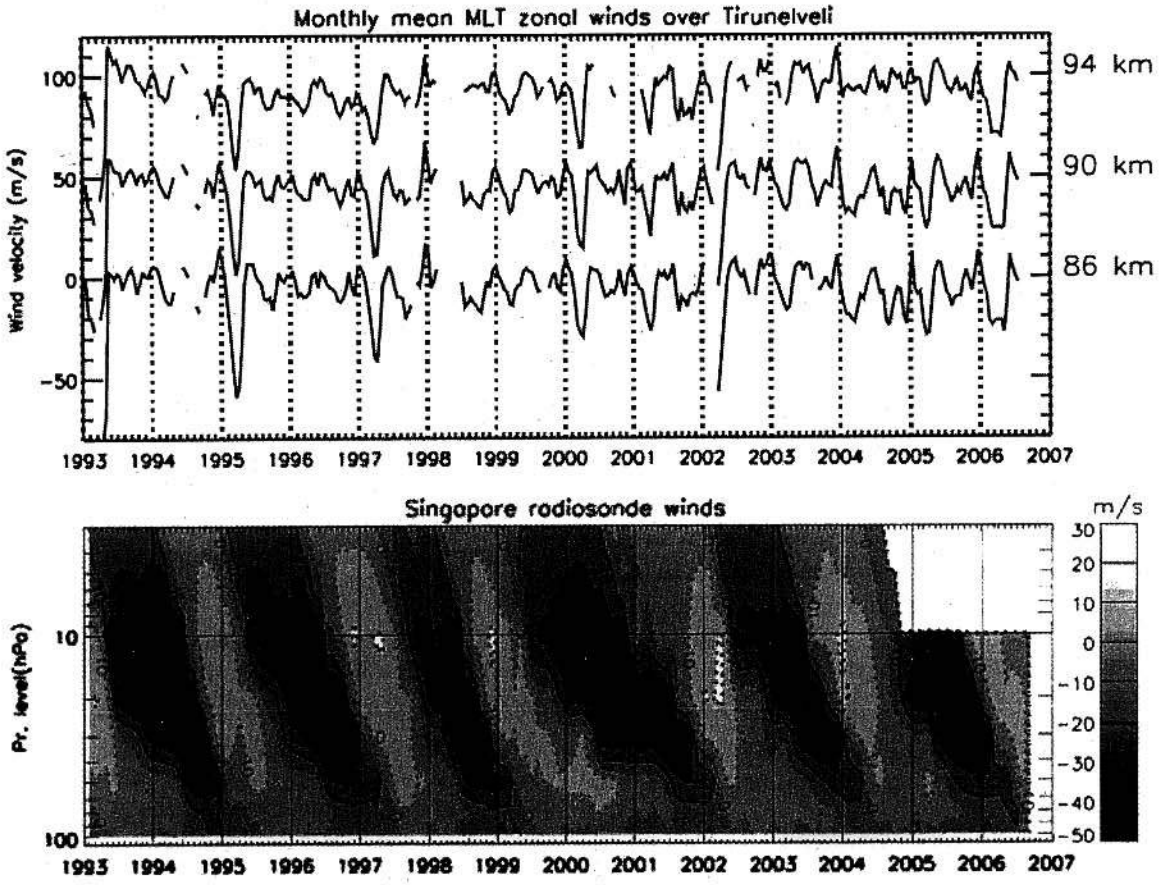

Fig. 1. Monthly mean zonal winds over Tirunelveli for heights 86, 90 and 94 km (top) and monthly mean zonal winds at pressure levels between 90 and 3 hPa over Singapore (bottom) (from Sridharan et al (2007)[23]).

A SKiYMET meteor radar system was installed at Trivandrum during mid-2004 and has been yielding reliable wind measurements in the height region 80-100 km since then. Following a novel method proposed by Hocking to compute the momentum fluxes of short-period gravity waves[24], a recent study made quantitative estimates of the gravity wave contribution to the easterly and westerly phases of the mesospheric SAO[25]. An earlier work that

the MLT region perhaps originates in the lower atmospheric convective activity through gravity wave excitation and in ISO modulated tropospheric water vapour heating[28].

The horizontal wind data acquired by MF radar at Tirunelveli (8.7°N, 77.8°E) were used in a recent work to study the long-term variability and trends in the MLT

winds[23]. The annual mean meridional winds over Tirunelveli revealed a monotonic change from northward to southward from the year 1993 to 2006. This result is in contrast to the results reported from mid-latitudes, where decreasing trend in the annual mean southward winds was noted.

Tides and Planetary Waves : Atmospheric tides have been studied very extensively in the past and a vast literature is available on the subject (Forbes, 1984, for a review[29]). Migrating tides are primarily driven by the absorption of solar radiation by water vapour in the troposphere (in the case of diurnal tides) and ozone in the stratosphere (in the case of semidiurnal tides). Non-migrating tides have their origin in land-sea contrast, non-uniform distribution of ozone and water vapour and latent heat release in deep tropical convective clouds[30]. Many ground and satellite-based observational studies in the past have indicated that the diurnal tide in the equatorial and low latitude MLT region undergoes large variations as a function of time, height, latitude and longitude. Model results attribute some of these variations to the variations in water vapour concentrations and clouds, variations in eddy dissipation, gravity wave interactions with the tide, planetary wave-tide interactions and latent heat release.

Single station studies on the characteristics and variabilities of the diurnal tide in the low latitude MLT region have been carried out using long-term observations over Christmas Island (2°N, 157°W)[31], Kauai (22°N, 160°W)[31], Jakarta (6.4°S, 106.7°E)[32] and Tirunelveli[33]. Long-term tidal wind observations from Jakarta have clearly indicated a tidal response to the El Nino Southern Oscillation event that occurred during 1997-1998[34]. In particular, the seasonal cycle in diurnal tide activity that shows a pronounced increase during local summer months over the Indonesian region is suppressed during the El Nino year when the deep convective activity shifts towards central and eastern Pacific. Fig. 2 shows the results obtained from this work. It has been suggested that the deep convective activity in the tropical troposphere generates non-migrating tides that propagate to the MLT heights and compete with the migrating tidal components to determine the overall behaviour of the diurnal tide at higher altitudes. The role of tropical convection and its time and spatial variations ascribed to large-scale air-sea interactions were thus shown to contribute to the observed interannual variability of the diurnal tide in the upper mesosphere. A recent theoretical work suggests a stronger migrating diurnal tidal forcing

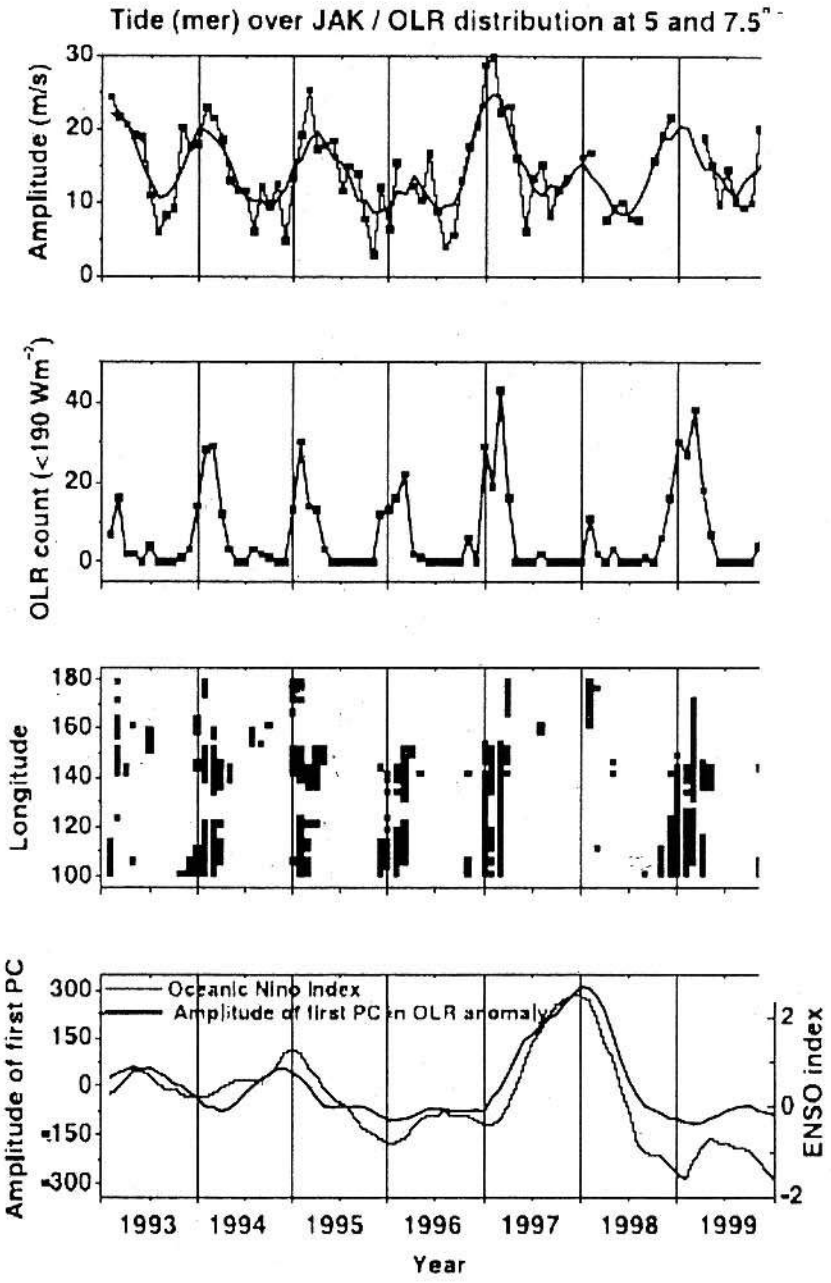

Fig. 2. Temporal variation of diurnal tide amplitude at 86 km over Jakarta (top), the OLR count (second plot) representing number of pixels on OLR maps for which the OLR brightness is less than 190 Wm^{-2} and the position of those pixels shown as longitudinal distribution in the range 100-180°E (third plot). The bottommost panel depicts the Oceanic Nino Index and the amplitude of the first principal component derived from the OLR anomaly (from Gurubaran et al. (2005)[34]).

because of the altered heating patterns in the Pacific and excitation of several weaker nonmigrating modes by latent heating thus emphasizing water vapour heating as the larger contributor to tidal enhancement that was observed over Kauai during 1997-1998[35].

An experimental campaign to investigate the tidal characteristics in the middle atmosphere over the low latitude Indian sector was conducted under the CAWSES-India programme during February-April 2006[36], involving the radar groups at Trivandrum, Tirunelveli and Gadanki . During this period, the fortnightly rocket launches carried out as part of the MIDAS programme were scheduled to provide 4-hourly altitude profiles of winds in the middle atmospheric height region (25-65 km). A remarkable feature in the rocket-derived phase profiles is the clear downward progression in both zonal and meridional components in the lower altitude region (25-40 km) yielding a vertical wavelength of ~15 km (Fig. 3). An important observational finding that emerged from this campaign is that the radar observations at Tirunelveli/Trivandrum indicated the presence of 15-20 day modulation of diurnal tide activity at MLT heights that correlate well with a similar variation in the Outgoing Longwave Radiance (OLR) fields in the western Pacific suggesting a possible link between the observed tidal variabilities and variations in the deep tropical convection through the nonmigrating tides it generates.

The planetary waves in the middle atmosphere belong to three categories: (1) normal modes, (2) forced modes and (3) equatorially trapped modes. Of these waves, the equatorial waves have gathered significant attention among the Indian scientific community in recent years[12]. The main conclusions that emerged out of these studies are: (1) Kelvin waves with periods shorter than ~9 days can penetrate into the mesosphere, whereas the longer period waves are confined to the stratosphere and below, (2) there is evidence of penetration of extratropical planetary wave activity into the tropical middle atmosphere, (3) the tropical tropopause is modulated by equatorial waves in the period range 4-15 days, (4) the gravity wave activity in the mesosphere is modulated by equatorial waves, (5) the vertical flux of horizontal momentum of the equatorial waves reveals equinoctial maximum and solstitial minima and (6) the vertical fluxes of the horizontal momentum of the equatorial waves are not adequate to account for the observed mean flow accelerations which result in the QBO and SAO. A 3.5-day ultra-fast Kelvin wave is often observed in the tropical MLT region that undergoes semi-annual variation at heights where the mesopause SAO in mean zonal wind peaks[37].

Satellite and ground-based radar observations reveal the presence of a 6.5-day wave which is a prominent dynamical feature of the MLT region[38,39,40]. The MF radar observations over Tirunelveli indicate an enhanced 6.5-day wave activity when the mean winds in the MLT region are eastward and reduced wave activity when the mean winds are westward[39]. It was earlier suggested that the 6.5-day wave is a manifestation of the Doppler shifted 5-day normal mode but this idea was soon discarded and the suggestion that a baroclinic or barotropic instability due to shears in winds or gradients in temperature could result in the preferential amplification of the 6.5-day wave was made[41]. A recent study made use of the National Center for Environmental Prediction (NCEP) reanalysis results at 10 hPa as lower atmospheric specifications in the National Center for Atmospheric Research thermosphere-ionosphere-electrodynamics general circulation model (NCAR TIME-GCM) and showed that the 6.5-day wave displays seasonal variations that are consistent with the satellite observations and that the wave response in the MLT is closely tied to the waveguide, the critical layer and the baroclinic/barotropic instability[42].

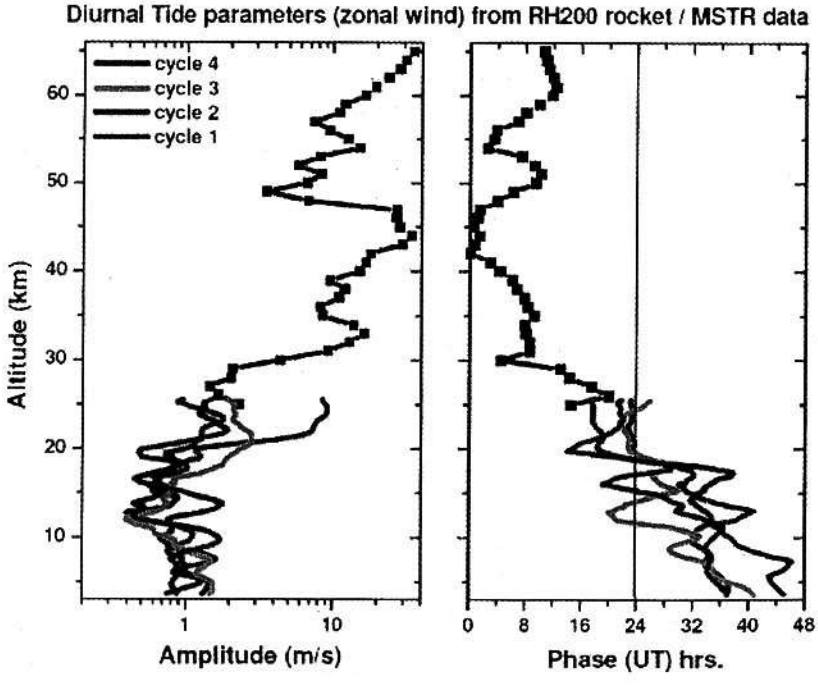

Fig. 3. Altitude profiles of amplitude and phase of the diurnal tide in zonal wind derived from the fortnightly rocket launches during February-April 2006 and MST radar derived parameters for the four cycles (shown in different colours) (from Gurubaran et al. (2008)[36]).

The thermal structure of the atmosphere is important for both the generation and propagation of atmospheric waves. Localized cooling, as for example, that can occur during solar eclipse, due to a reduction in the absorption of solar UV radiation, can result in wave perturbations. Using lidar observed temperatures over Gadanki, a 4-day wave was shown to occur accompanying an anomalous stratospheric cooling[43]. The lidar observations from the same site reveal a modulation of gravity waves by the equatorially trapped Kelvin waves of period ~12 days[44]. Radiosonde observations made at several sites in the Indian peninsular region suggest the role of Kelvin waves in producing low tropopause temperatures through a modulation of the tropopause height and temperature thereby participating in the 'freeze-dry' process of tropospheric air intruding into the stratosphere[45].

Gravity waves : Gravity wave investigations of the tropical lower and middle atmosphere that took place in India in recent years have been made using the MST radar at Gadanki[46,47], lidar observations at Gadanki[48], balloon and rocket soundings at Thumba[13], MF/meteor radar observations at Tiruhelveli[26]/Trivandrum[25] and all-sky imaging observations from Kolhapur[49].

Well-planned experiments with the MST radar at Gadanki had provided several insights of convectively generated gravity waves. These waves typically have periods of a few tens of minutes with a horizontal wavelength of a few tens to a few hundreds of kilometres[50]. It has been observed that during an actively convective period, the signal-to-noise ratio (SNR) for the vertical beam that represents the radar backscattered echo power maximized around the tropopause along with enhancements in spectral width indicating enhanced turbulence[46] (refer to Fig. 4). The tropopause is often observed to weaken due to mixing induced by penetrating convection. From the perturbations in vertical wind velocities, gravity waves can be identified. Phase profiles of dominant short-period waves clearly indicate the presence of source regions occurring at heights of ~12 km[47].

Rayleigh lidar observations at Gadanki were used in a recent study to characterize the gravity wave spectrum in the stratosphere and mesosphere (30-70 km)[51]. Significant differences were noticed between the computed wavenumber spectra and wavenumber spectra derived from a saturated gravity wave model. Mesospheric temperature inversions have often been observed over Gadanki in the recent past[52]. The occurrence frequency of the inversion showed semiannual variation with maxima in the equinoxes and minima in the summer and winter, which was quite different from that reported for the midlatitudes. This

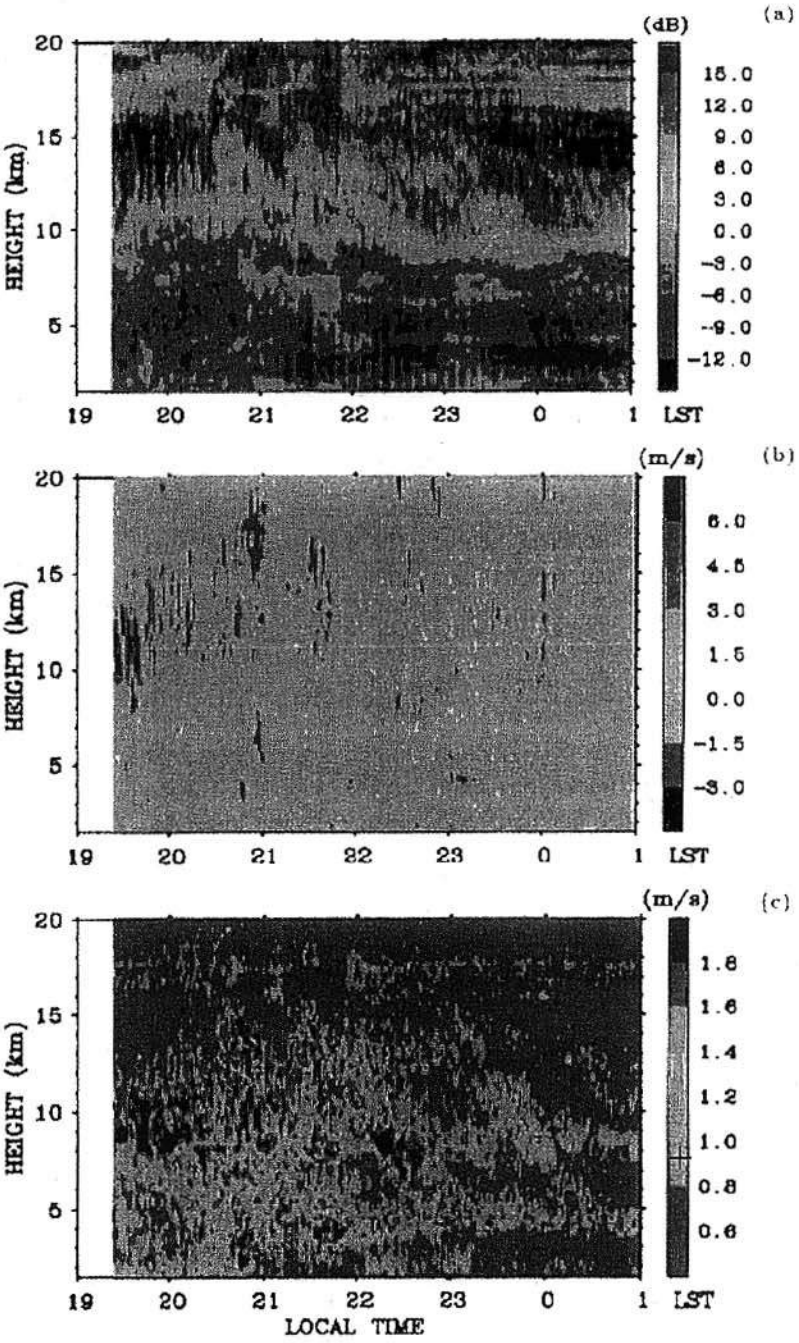

Fig. 4. MST radar observations from Gadanki: (a) SNR, (b) vertical wind velocity (positive indicates updrift and negative values indicate downdrift), and (c) Doppler width (from Dhaka et al.(2002)[46]).

seasonal dependence in the temperature inversions has been attributed to the seasonal behaviour of the gravity wave activity over this low latitude station that is expected to show maxima during equinoxes. In a separate study that made use of the MST radar echoes over Gadanki, summertime maxima in turbulent energy dissipation rates and eddy diffusion coefficients were observed at mesospheric heights which are presumed to be related to the enhanced gravity activity that would have occurred during the Indian summer monsoon[53].

Two separate studies were carried out recently using the long-term MST radar observations from Gadanki. One study examined the vertical wavenumber spectra and their seasonal variabilities in the tropical troposphere and compared them with the wavenumber spectra predicted by gravity wave saturation theory[54]. The differences between the observed and theoretical wavenumber spectra were attributed to the seasonal dependence of buoyance frequency and mean winds and their shears. The monthly mean gravity wave spectra retrieved in this study serve as a means for representing gravity wave characteristics in atmospheric models. Another study that used long-term MST radar observations explored the potential source mechanisms for the generation of inertia-gravity wave activity over Gadanki[55].

Low-intensity CCD images of the nightglow emissions provide an excellent means of detecting two-dimensional spatial and temporal evolution of short-period gravity waves over a large geographic area with high temporal resolution. The operation of an all-sky airglow imager yields important information on the occurrence frequency, horizontal wavelengths, and apparent horizontal phase velocities of the wave perturbation[49]. From an observational campaign conducted at Panhala (17.0°N, 74.2°E), the observed horizontal phase speed (~ 50 m/s), wavelength (~25 km), wave period (~8 min), of the gravity waves have been determined from a set of sequential images of OI 557.7 nm emissions that occur at 97 km and OH emissions emanating from 87 km[49]. All-sky airglow imagers were deployed at Tirunelveli during January 2007 and at Allahabad a year later. A variety of wave events like bands (quasi-monochromatic waves), fronts (bores) and ripples were detected during campaigns conducted at Tirunelveli, Kolhapur and Allahabad.

Sudden stratospheric warming and its signatures at low latitudes : Sudden stratospheric warming (SSW) is a major atmospheric disturbance of high latitude origin whose signatures in the low latitude MLT region are only beginning to be understood. One study that utilized temperature observations from the Wind Imaging Interferometer (WINDII) and Microwave Limb Sounder (MLS) experiments on the Upper Atmosphere Research Satellite (UARS) satellite and the Sounding the Atmosphere using Broadband Emission Radiometry (SABER) experiment on the Thermosphere, Ionosphere, Mesosphere Energetics and Dynamics (TIMED) satellite during the winters of 1992-1993, 1993-1994 and 2003-2004, took note of mesospheric cooling at low latitudes at the time of stratospheric warming[56]. Planetary waves at periods 7 and 16 days were found to be enhanced during the observed warming events.

It has been noted that no major stratospheric warming occurred during the years 1993-1998, whereas several major warming events occurred after 1998. The wind variances due to gravity waves of periods 2-6 hours in the height region 84-98 km over Tirunelveli, during 2005-06 were observed to be enhanced around the day of onset of an SSW event and this persisted after the end of the event. An enhancement of gravity wave variances was observed during most of later winter and early spring equinox that follows major mid winter SSW events[57].

Mesosphere-lower thermosphere-ionosphere (MLTI) coupling : The mesosphere - lower thermosphere region is a critical transition region that is coupled not only to the lower atmosphere below but also to the ionized regions above. Neutral dynamics, electrodynamics and photochemistry are the governing processes within the MLTI region that are largely coupled. For example, the wind dynamo that operates at heights where ionospheric conductivities maximize is responsible for the generation of electrostatic fields and current systems. The photodissociation products (atomic oxygen, for example) having their origin in the lower thermosphere and carrying significant chemical energy can be transported to mesospheric altitudes where the excess energy is converted to heat that in turn influences the dynamics at these heights. It has been predicted that the mesosphere and thermosphere will cool in response to the tropospheric anthropogenic changes (increase of methane, for example).

A primary motivation for the Indian scientific community to address the MLTI coupling related aspects is the need to explain the day-to-day variabilities of several ionospheric parameters observed at and close to the magnetic equator. For example, the day-to-day variability noticed in the daily magnetic records obtained from a dip equatorial station even during magnetically quiet times has baffled the investigators for several decades. The occurrence of equatorial spread F on one day and its non-occurrence on another day within a same season are yet to be explained satisfactorily. Only recently, the influence of waves and tides in controlling the day-to-day variability

of the electrodynamics of equatorial ionospheric regions has become a topic of great interest[58].

The Indian contributions to this area so far have primarily emerged from the use of geomagnetic data, MLT radar observations and photometric observations of airglow emissions. MF radar observations from Tirunelveli had contributed in two studies that assessed the role of tides and planetary waves in causing the variabilities of the equatorial electrojet (EEJ)[59,60]. Whereas one study found significant correlation between the occurrence times of the quasi-2-day planetary wave at mesospheric altitudes and 2-day oscillations in EEJ strength[59], the other study emphasized the variability of tidal modes and their interplay in the evolution of EEJ whose extreme manifestation in ground geomagnetic field variations is the reversal of the electrojet in the afternoon hours[60].

The unique dayglow photometers developed in India had been successfully used for making daytime mesopause temperature measurements over the Indian longitudes in recent years[7]. A variety of studies carried out with the dayglow photometers had provided for the first time useful glimpses of the behaviour of the mesopause temperatures and energetics and dynamics driving the low latitude MLTI region. For example, a quasi16-day oscillation noticed simultaneously in the hydroxyl dayglow intensities and zonal wind at ~87 km indicates the presence of a quasi 16-day wave at mesopause heights possibly of lower atmospheric origin[61]. A later study found a quasi 16-day oscillation in daytime mean mesopause temperature and ground geomagnetic field variations during a different period[62]. The planetary wave is found to maximize in amplitude during January-March months, and to modulate the mesopause temperature, zonal wind, duration and peak of EEJ, nearly simultaneously. The wave-tidal interactions and subsequent modification in the diurnal tide have been suggested to be responsible for the observed variations.

Another study using the dayglow photometer with a unique meridional scanning capability provided evidence for a lowering of the mesopause temperature in the afternoon hours during the counter electrojet[63]. A lowering of temperature by as much as ~25 K was observed during certain CEJ events, which includes a few partial CEJs (refer

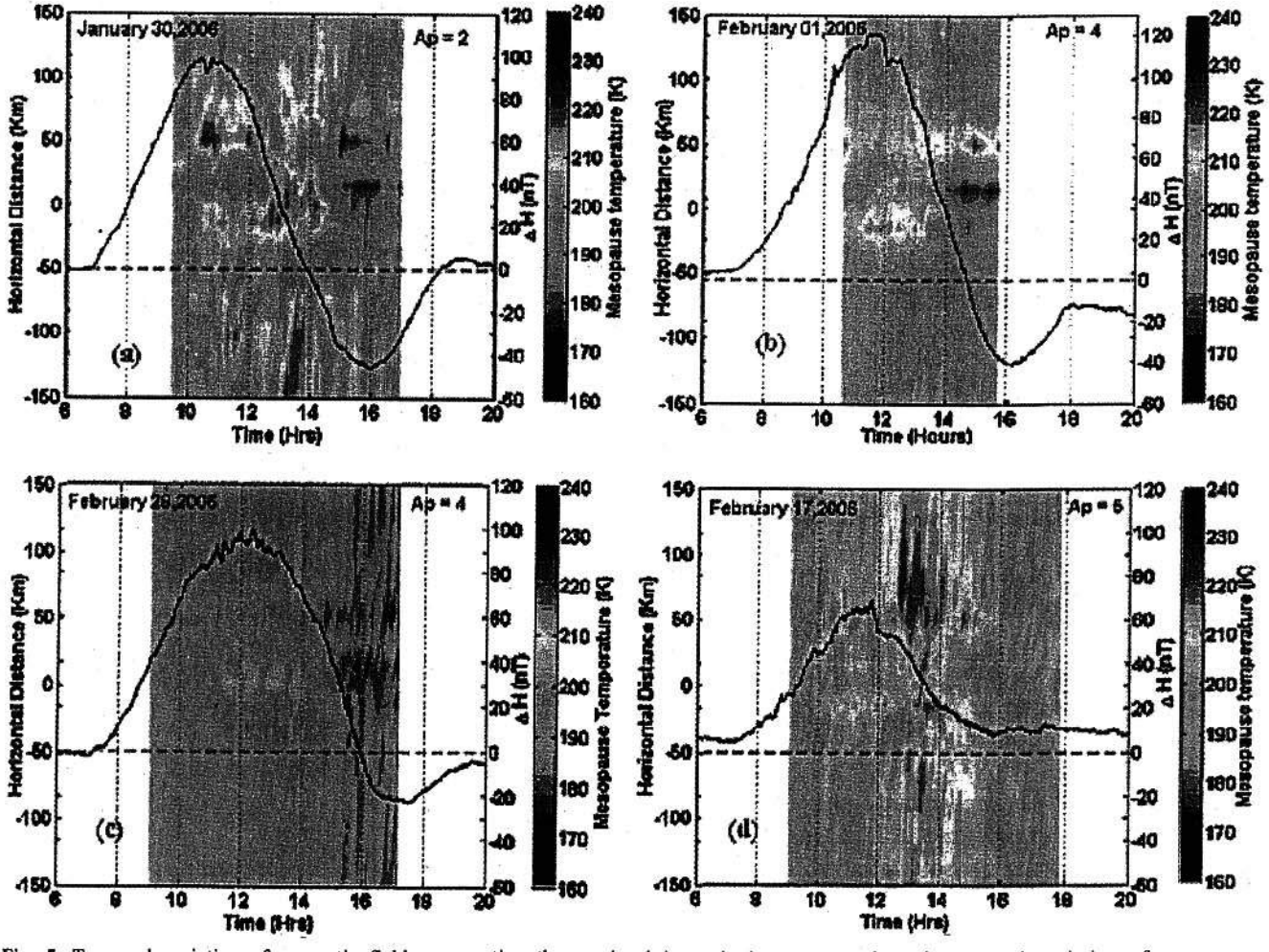

Fig. 5. Temporal variation of magnetic field representing the overhead ionospheric current and spatio-temporal variation of mesopause temperature on three CEJ days and one normal electrojet day (from Vineeth et al. (2007)[63]).

to Fig. 5). Gravity wave-tidal interaction through vertical upward wind has been hypothesized to manifest as lowering of mesopause temperature and also as CEJ.

The nighttime photometric observations of OH airglow emissions from Kolhapur had yielded temperatures of the mesopause region between 2002 and 2005 contributing to the study of energetics and dynamics from this low latitude site[64,65]. A recent work has compared the rotational temperatures measured with the photometer and the temperatures retrieved by the SABER instrument on board the TIMED satellite and the agreement has been found to be good.

Studies of the Upper Atmosphere

Ionospheric irregularities : Plasma instabilities in the equatorial ionosphere produce inhomogeneities or irregularities in the plasma density, which are capable of scattering incoming radio signals and thus affect the operation of satellite-based communication and navigation systems such as GPS. In the night-time equatorial ionosphere, the irregularities are referred to as equatorial spread-F (ESF) and have been the subject of intense experimental and theoretical investigations during recent times[66]. Recently the observations of magnetic field fluctuations associated with equatorial ionospheric plasma bubbles (EIPBs) have led to new theories [67,68], and provided a new tool for studying the spatial evolution of EIPBs both under geomagnetically quiet and disturbed periods. The question of whether EIPBs and associated ESF irregularities observed by ground-based radio techniques such as ionospheric scintillation or radar observations are generated freshly above the observation point or they have simply drifted from another location where they may have been generated several hours earlier has also been investigated[69], since this is important for establishing how geomagnetic activity influences the development of EIPBs. Based on this idea, spaced receiver scintillation observations were used to identify nascent EIPBs generated after 22LT due to magnetic activity[70].

The ionograms recorded at the equatorial station, Tirunelveli (77.8°E, 8.7° N, dip lat.0.7°N),using a newly installed CADI (Canadian Advanced Digital Ionosonde) have been analyzed to study the occurrence and other properties of an additional ionospheric layer known as F3 layer[71]. Normally the layer was observed between 08:30 to 11:30 hrs LT with rare exceptions. The duration of occurrence varied from 15 minutes to 2 hours. The F3 - layer was observed more frequently in summer than in winter.

The recent development of highly sensitive cooled CCD cameras has made it possible to measure very faint emissions in airglow in more detail [72,73,74]. A CCD based all sky imager with 180° field of view has been operating at Kolhapur (16.8° N, 74.2° E, dip latitude 10.6° N) and Panhala in India on clear moon less nights to study the dynamics in the mesopause and F-region of the ionosphere. The imager has the capability of permitting observations over regions covering several million square kilo meters from a single observing station. It was observed that a large number of EIPB events are characterized by the development of strong Equatorial Ionization Anomaly (EIA). Two examples of equatorial movement of the Appleton Anomaly crests (reverse ionization anomaly) with speed of 36-40 m/s on the night of Jan 26, 1998 (Fig. 6) and January 18, 1999 during the observation of ionospheric plasma bubbles have been reported showing the observed correlation between EIA and bubbles[72]. The first visual representation of the reverse equatorial plasma fountain during nighttime was made from Mt. Abu using images obtained by an All Sky Imaging Fabry-Perot Spectrometer[75,76] observing the OI 630.0 nm airglow emission line. From the identifiable features when the enhanced airglow emitting region moved overhead and when it completely left the field-of-view, the equator-ward

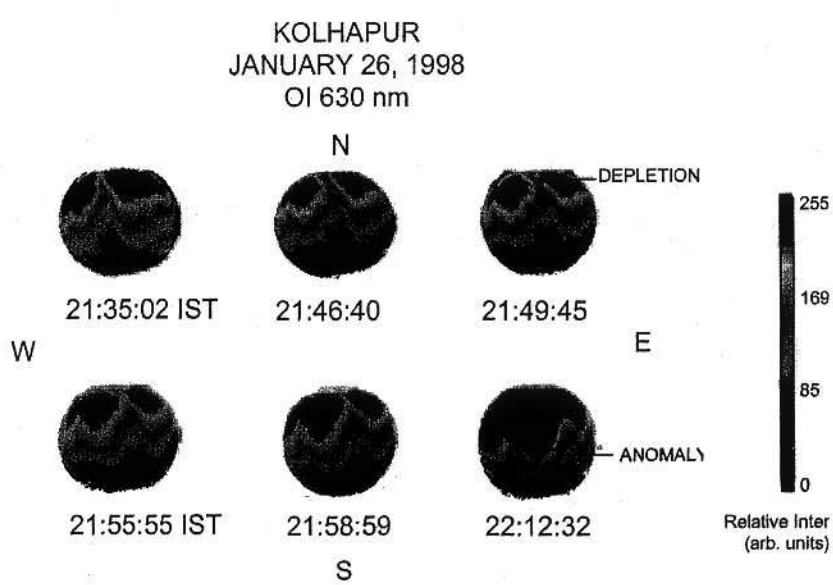

Fig. 6. Movement of the reverse ionization anomaly with drift speeds of 36-40 m/s on the night of January 26, 1998. Note also the eastward movement of the bubble along with its vertical rise in altitude extending increasingly northward (from Mukherjee (2002) [72]).

velocity of the equatorial ionization anomaly (EIA) was estimated to be ~150 km/hr.

The ionospheric plasma bubbles manifest in all sky imaging observations at Kolhapur as nearly north-south aligned intensity depleted regions[73] (Fig. 7). The all-sky images permitted the determination of the plasma drift velocities, depth and width of the plasma bubbles. Also, the observed zonal plasma bubble drift velocities have been compared with the thermospheric zonal neutral wind velocities obtained from the HWM-93 model showing good agreement[73,74]. The simultaneous depletions in OI 630.0 nm, OI 557.7 nm and OI 777.4 nm emissions were also observed [73]. The overall intensity of the OI 777.4 nm emission is found to be much weaker than that of OI 630.0 nm emission. The images of three oxygen lines show more or less similar structures. It is inferred from the all-sky images that the corresponding plasma depleted flux tube crosses the magnetic equatorial plane at an altitude above 1500 km [73].

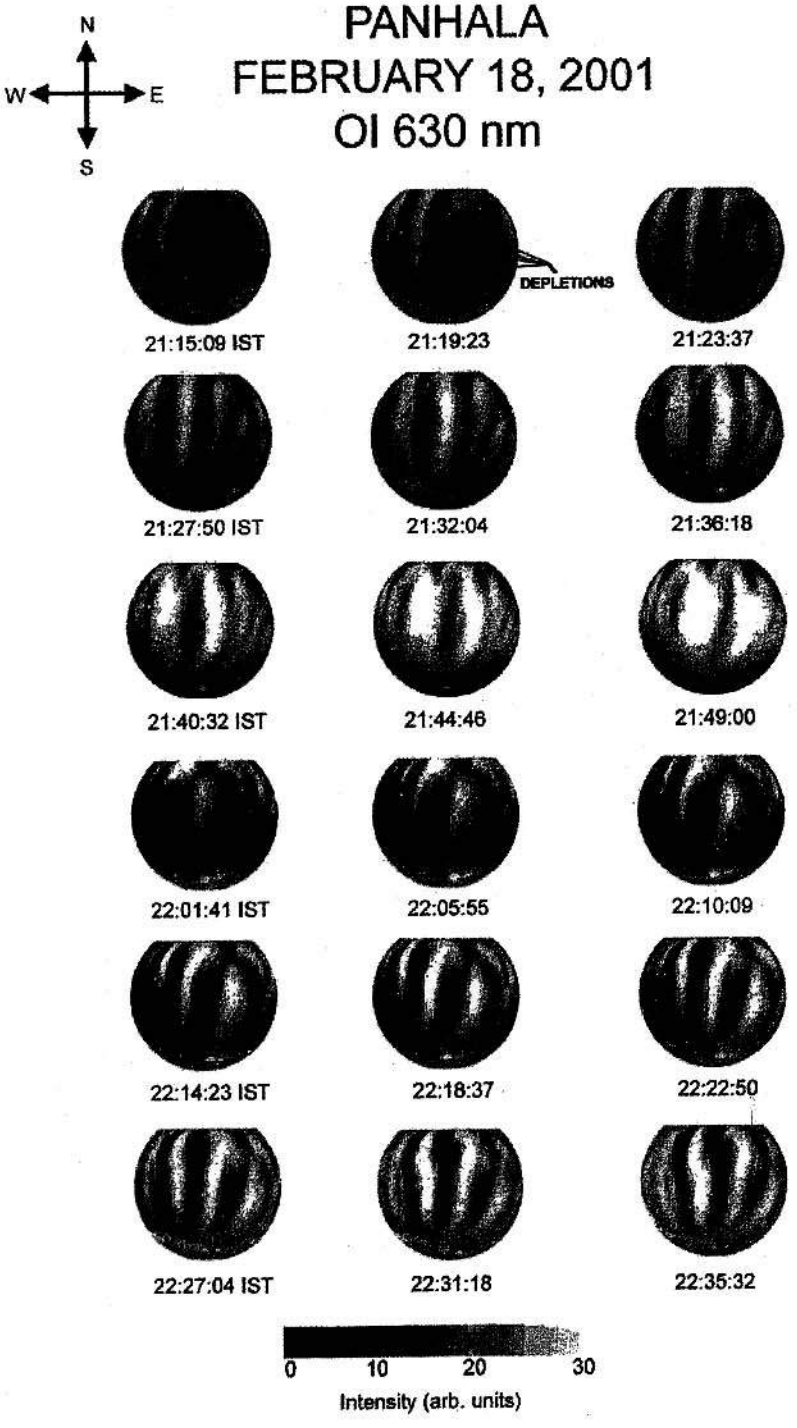

Fig. 7. OI 630.0 nm images obtained at Panhala on the night of February 18, 2001 showing north-south aligned plasma bubbles (from Harikishore et al.(2007)[73]).

Effects of Magnetic Storms on Airglow emissions : The characteristics of night airglow variations observed during the period of a moderate/weak geomagnetic storm of February 5-7, 2000 with SSC (Storm Sudden Commencement) commencing at 15:42 UT (21:12 IST (Indian Standard time) = UT+5.4 hrs) on February 5, 2000 have been brought out[77] by studying the images of various emissions. The images on the night of February 6, 2000 show the development of strong ionization anomaly (EIA) with bright intensity regions in OI 630.0 nm and the signature of rising bubbles with very low intensity. Though the signature of ionospheric plasma bubbles were not observed on the night of February 7, 2000 the OI 630-nm images showed the presence of large scale enhanced airglow moving to the south-east direction (Fig. 8). The speed was significantly fast (~ 300 m/s). There were bright intensity regions also observed in OI 557.7-nm airglow, but no intensity enhancement was seen in other mesospheric emissions (Na (589.3-nm) and hydroxyl (OH) airglow) during this magnetic disturbance. The ionosonde observations at the nearby station, Visakhapatnam (lat. 17.67° N, long. 83.32° E) also showed enhancement in electron density parameter ((foF2) ^{2}) at the station on each night compared to the night of February 4-5 (quiet day) around the same time interval maximizing around 23:00 IST on the night of February 7, 2000. However, noontime TEC values were enhanced on February 6 and 7, 2000 with maximum occurring on February 7, 2000. The enhanced storm time effects in the ionosphere were

mainly confined to the low latitude region, the effects were subdued in the mid latitude stations.

Correlation of Airglow and Radar Observations : The first simultaneous observations of temporal and spatial structures of plasma bubble using an airglow imager and radar have been reported from Indian longitude sector[78]. The observations were made on a number of nights in March-April, 1998-1999 with an All-sky imager from Kolhapur (16.8° E, 74.2° E, dip latitude 10.6° N), which observed OI 630.0 nm airglow depletions due to equatorial plasma bubbles and 53 MHz MST Radar from Gadanki (13.5° N, 79.2° E, dip latitude 6.3° N) providing backscatter from small scale irregularities associated with ESF. During this campaign, a digital ionosonde from Sriharikota, a station near Gadanki, and another one from Trivandrum, a magnetically equatorial station, were also operational to monitor ionospheric conditions. Wave-like variations in bottomside structure and vertically rising plume structures in the height region 350-550 km were observed in height-time-intensity maps of radar echoes. It is noted that the plumes observed by the radar coincide well with the airglow depletions. Further, the most intense radar backscatter matches well with the deepest depletion in OI 630.0 nm airglow intensity. A most important observation that comes from the radar observations is the occurrence of a large number of plumes over Gadanki as against that of Jicamarca. This assumes special significance since it raises the question whether the larger number of plumes is associated with greater gravity wave activity. Another interesting observation is that the irregularity velocities in the bottomside structures are predominantly downward with values sometimes reaching 100 m s^{-1}. Considering that the airglow intensity is proportional to electron density, these observations can be viewed as depletion/ enhancement in plasma density[78].

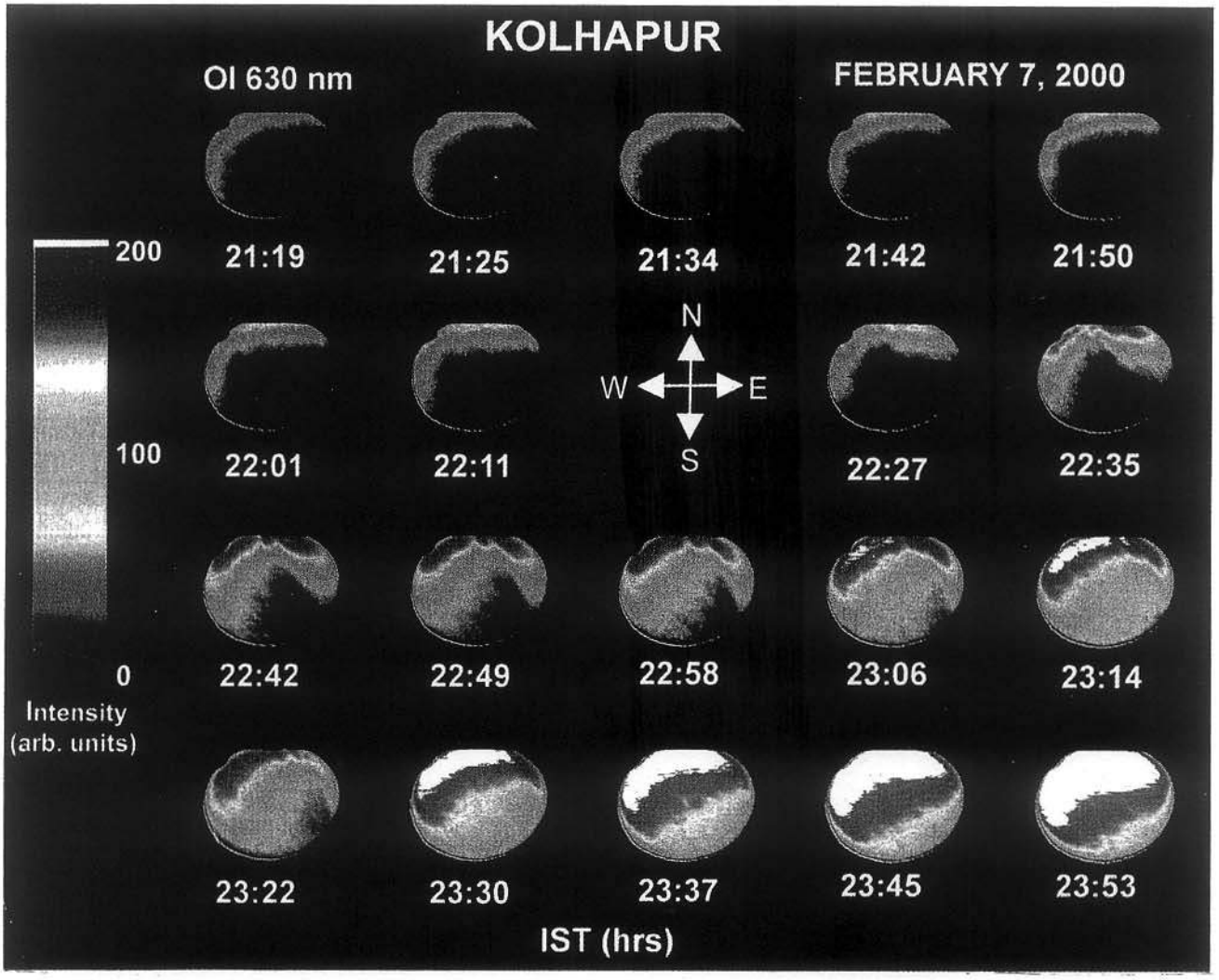

Fig. 8. All-sky images (180° field of view) of OI 630- nm on the night of February 7, 2000 at Kolhapur showing severe enhancement in OI 630-nm night airglow in the northern sky from 22:11 IST onwards maximizing at 23:53 IST(from Mukherjee (2006)[77]).

Observation of MTM phenomena : A combination of in-situ satellite measurements and ground based experiments in the last three decades has revealed many new features of the equatorial ionosphere. There are cases when the measurements both by ground-based and satellite borne instrumentation, revealed a pronounced increase in the neutral temperature around mid-night over the equator, sometimes the value exceeding the afternoon maximum[79]. This feature is known as the midnight temperature maximum (MTM), a region of anomalous temperature and density that is generally considered to result from atmospheric tidal interactions. This influences very strongly the neutral thermospheric dynamics and the neutral plasma. The characteristics of MTM (such as shape, amplitude, the time of occurrence and propagation) are highly variable. Winds generated due to pressure bulge phenomena propagate pole ward (northward) and its vertical component moves the F-region plasma downward to region of enhanced loss and airglow production.These characteristics were observed in the all-sky images and photometric data of OI 630 nm at Kolhapur showing the enhancement in intensity around 0200-0400 hrs IST and their subsequent propagation towards the north that may be due to signature of MTM [74,80]. At the same time, the ionosonde data from Visakhapatnam, Sriharikota and Trivandrum showed a decrease in height (h'F) of the F-region, which is known as the collapse of the F-layer. The computed values from servo model [81] for meridional component of wind velocity at the station also showed enhancement varying between 91 m/s and 201m/s, which was more than the normally observed values at the low latitude region. The temperature enhancement[82] over Kovalur, India was found to be consistent with the MTM observation at Jicamarca. ❐

References

1. J. M. Forbes, *J. Geomag. Geoelectr.* **48**, 91-98 (1996).
2. J. W. Meriwether Jr., *J. Geophys. Res.* **94**, 14, 629-14, 646 (1989).
3. C. G. Fesen, G. Crowley, R. G. Roble, A. D. Richmond, and B. G. Fejer, *Geophys. Res. Lett.* **27**, 1851-1854 (2000).
4. M. E. Hagan, A. Maute, R. G. Roble, A. D. Richmond, T. J. Immel, and S. L. England, *Geophys. Res. Lett.* **34**, L20109, doi:10.1029/2007GL030142 (2007).
5. M. A. Abdu, *J. Atmos. Sol. Terr. Phys.* **59**, 1505-1519 (1997).
6. A. Coster and A. Komjathy, *Space Weather* **6**, S06D04, doi:10.1029/2008SW00400 (2008).
7. T. K. Pant, D. Tiwari, C. Vineeth, S. V. Thampi, S. Sridharan, C. V. Devasia, R. Sridharan, S. Gurubaran, and R. Sekar, *Geophys. Res. Lett.* **34**, L15102, doi:10.1029/2007GL030193 (2007).
8. A. Taori, R. Sridharan, D. Chakrabarty, R. Narayanan, and P. V. S. Ramarao, *Geophys. Res. Lett.* **28**, 1387-1390 (2001).
9. A. K. Patra, D. Tiwari, S. Sripathi, P. B. Rao, R. Sridharan, C. V. Devasia, K. S. Viswanathan, K. S. V. Subbarao, R. Sekar, and E. A. Kherani, *J. Geophys. Res.* **110**, A02307, doi:10.1029/2004JA010565 (2005).
10. D. Tiwari, B. Engavale, A. Bhattacharyya, C. V. Devasia, T. K. Pant, and R. Sridharan, *Ann. Geophys.* **24**, 1419-1427 (2006).
11. C. A. Reddy, C. Raghava Reddi and K. G. Mohankumar, *Quart. J. R. Met. Soc.* **112**, 811-823 (1986).
12. M. N. Sasi, *Curr. Sci.* **89**, 475-487 (2005).
13. G. Ramkumar, T. M. Antonita, Y. Bhavani Kumar, H. Venkata Kumar, and D. Narayana Rao, *Ann. Geophys.* **24**, 2471-2480 (2006).
14. M. P. Baldwin, L. J. Gray, T. J. Dunkerton, K. Hamilton, P. H. Haynes, W. J. Randel, J. R. Holton, M. J. Alexander, I. Hirota, T. Horinouchi, D. B. A. Jones, J. S. Kinnersley, C. Marquadt, K. Sato and M. Takahashi, *Rev. Geophys.* **39**, 179-229 (2001).
15. J. R. Holton and R. S. Lindzen, *J. Atmos. Sci.* **29**, 1076-1080 (1972).
16. T. M. Antonita, G. Ramkumar, K. Kishore Kumar, and S. V. Sunil Kumar, *Geophys. Res. Lett.* **35**, L09805, doi:10.1029/2008GL033960 (2008).
17. R. J. Reed, *J. Geophys. Res.* **71**, 4223-4233 (1966).
18. I. Hirota, *J. Atmos. Sci.* **35**, 714-722 (1978).
19. V. Deepa, G. Ramkumar, and B. V. Krishna Murthy, *Ann. Geophys.* **24**, 2481-2491 (2006).
20. T. M. Antonita, G. Ramkumar, K. Kishore Kumar, K. S. Appu, and K. V. S. Nambhoodiri, *J. Geophys. Res.* **112**, D12115, doi:10.1029/2006JD008250 (2007).
21. R. Rajaram and S. Gurubaran, *Ann. Geophys.* **16**, 197-204 (1998).
22. M. D. Burrage, R. A. Vincent, H. G. Mayr, W. R. Skinner, N. F. Arnold, and P. B. Hays, *J. Geophys. Res.* **101**, 12,847-12,854 (1996).
23. S. Sridharan, T. Tsuda, and S. Gurubaran, *J. Geophys. Res.* **112**, D23105, doi:10.1029/2007JD008669 (2007).
24. W. K. Hocking, *Ann. Geophys.* **23**, 1-7 (2005).
25. T. M. Antonita, G. Ramkumar, K. Kishore Kumar and V. Deepa, *J. Geophys. Res.* **113**, D10115, doi:10.1029/2007JD009089 (2008).
26. S. Gurubaran and R. Rajaram, *J. Geophys. Res.* **106**, 31,817-31,824 (2001).
27. S. D. Eckermann, D. K. Rajopadhyaya, and R. A. Vincent, *J. Atmos. Terr. Phys.* **59**, 603-627 (1997).
28. K. Kishore Kumar, T. M. Antonita, G. Ramkumar, V. Deepa, S. Gurubaran, and R. Rajaram, *J. Geophys. Res.* **112**, D07109, doi:10.1029/2006JD007962 (2007).
29. J. M. Forbes, *J. Atmos. Terr. Phys.*, **46**, 1049-1067 (1984).
30. M. Hagan, Geophys. Monogr., **123**, pp.177-190, (2000). edited by D. E. Siskind, S. D. Eckermann and M. E. Summers, AGU, Washington, D.C.

31. Vincent, R. A., S. Kovalam, D. C. Fritts and J. R. Isler, *J. Geophys. Res.* **103**, 8667-8683 (1998).

32. Tsuda, T., K. Ohnishi, F. Isoda, T. Nakamura, R. A. Vincent, I. M. Reid, S. W. B. Harijono, T. Sribimawati, A. Nuryanto, and H. Wiryosumarto, *Earth Planets Space* **51**, 579-592 (1999).

33. S. Gurubaran and R. Rajaram, *Geophys. Res. Lett.* **26**, 1113-1116 (1999).

34. S. Gurubaran, R. Rajaram, T. Nakamura, and T. Tsuda, (ENSO), *Geophys. Res. Lett.* **32**, L13805, doi:10.1029/2005GL022928 (2005).

35. R. S. Lieberman, D. M. Riggin, D. A. Ortland, S. W. Nesbitt, and R. A. Vincent, *J. Geophys. Res.* **112**, D20110, doi:10.1029/2007JD008578 (2007).

36. S. Gurubaran, D. Narayana Rao, G. Ramkumar, T. K. Ramkumar, G. Dutta, and B. V. Krishna Murthy, *Ann. Geophys.* **26**, 2323-2331 (2008).

37. S. Sridharan, S. Gurubaran and R. Rajaram, *J. Atmos. Solar-Terr. Phys.* **64**, 1241-1250 (2002).

38. E. R. Talaat, J. H. Yee and X. Zhu, *J. Geophys. Res.* **107**, 4133, doi:10.1029/2001/JD000822 (2002).

39. S. Sridharan, S. Gurubaran and R. Rajaram, *Earth Planets Space* **55**, 687-696 (2003).

40. P. Kishore, S. P. Namboothiri, K. Igarashi, S. Gurubaran, S. Sridharan, R. Rajaram and M. Venkat Ratnam, *J. Atmos. Solar-Terr. Phys.* **66**, 507-515 (2004).

41. C. K. Meyer and J. M. Forbes, *J. Geophys. Res.* **102**, 26, 173-26, 178 (1997).

42. H.-L. Liu, E. R. Talaat, R. G. Roble, R. S. Lieberman, D. M. Riggin, and J.-H. Yee, *J. Geophys. Res.* **109**, D21112, doi:10.1029/2004JD004795 (2004).

43. V. Deepa, G. Ramkumar and K. K. Kumar, *Ann. Geophys.* **25**, 1959-1965 (2007).

44. K. Parameswaran, K. Rajeev, M. N. Sasi, G. Ramkumar, and B. V. Krishna Murthy, *Geophys. Res. Lett.* **29**, 1077, doi:10.1029/2001GL013625 (2002).

45. A. R. Jain, S. S. Das, T. K. Mandal and A. P. Mitra, *J. Geophys. Res.* **111**, D07106, doi:10.1029/2005JD005850 (2006).

46. S. K. Dhaka, R. K. Choudhary, S. Malik, Y. Shibagaki, M. D. Yamanaka, and S. Fukao, *Geophys. Res. Lett.* **29**, 1872-1875 (2002).

47. K. K. Kumar, *Geophys. Res. Lett.* **33**, L01815, doi:10.1029/2005GL024109 (2006).

48. K. Rajeev, K. Parameswaran, M. N. Sasi, G. Ramkumar and B. V. Krishna Murthy, *J. Geophys. Res.* **108**, 4749, doi:10.1029/2003JD003682 (2003).

49. G. K. Mukherjee, *J. Atmos. Solar-Terr. Phys.* **65**, 1329-1335 (2003).

50. S. K. Dhaka, P. K. Devarajan, Y. Shibagaki, R. K. Choudhary and S. Fukao, *J. Atmos. Solar-Terr. Phys.* **63**, 1631-1642 (2001).

51. V. Sivakumar, P. B. Rao and H. Bencherif, *Ann. Geophys.* **24**, 823-834 (2006).

52. V. Sivakumar, Y. Bhavani Kumar, K. Raghunath, P. B. Rao, M. Krishnaiah, K. Mizutani, T. Aoki, M. Yasuai and T. Itabe, *Ann. Geophys.* **19**, 1039-1044 (2001).

53. M. N. Sasi and L. Vijayan, *Ann. Geophys.* **19**, 1019-1025 (2001).

54. A. Narendra Babu, K. Kishore Kumar, G. Kishore Kumar, M. Venkat Ratnam, S. Vijaya Bhaskara Rao, and D. Narayana Rao, *Ann. Geophys.* **26**, 1671-1680 (2008).

55. M. Venkat Ratnam, A. Narendra Babu, V. V. M. Jagannadha Rao, S. Vijaya Bhaskar Rao, and D. Narayana Rao, *J. Geophys. Res.* **113**, D07109, doi:10.1029/2007JD008986 (2008).

56. M. G. Shepherd, D. L. Wu, I. N. Fedulina, S. Gurubaran, J. M. Russell, M. G. Mlynczak and G. G. Shepherd, *J. Atmos. Solar-Terr. Phys.* **69**, 2309-2337 (2007).

57. S. Sathishkumar and S. Sridharan, *Geophys. Res. Lett.* **36**, L07806 doi: 10.1029/2008GL037081 (2009).

58. M. A. Abdu, T. K. Ramkumar, I. S. Batista, C. G. M. Brum, H. Takahashi, B. W. Reinisch, and J. H. A. Sobral, *J. Atmos. Solar-Terr. Phys.* **68**, 509-522 (2006).

59. S. Gurubaran, T. K. Ramkumar, S. Sridharan, and R. Rajaram, *J. Atmos. Solar-Terr. Phys.* **63**, 813-821 (2001).

60. S. Sridharan, S. Gurubaran and R. Rajaram, *J. Atmos. Solar-Terr. Phys.* **64**, 1455-1463 (2002).

61. T. K. Pant, D. Tiwari, S. Sridharan, R. Sridharan, S. Gurubaran, K. S. V. Subbarao and R. Sekar, *Ann. Geophys.* **22**, 3299-3303 (2004).

62. C. Vineeth, T. K. Pant, C. V. Devasia, and R. Sridharan, *Geophys. Res. Lett.* **34**, L12102, doi:10.1029/2007GL030010 (2007).

63. C. Vineeth, T. K. Pant, C. V. Devasia, and R. Sridharan, *Geophys. Res. Lett.* **34**, L14101, doi:10.1029/2007GL030298 (2007).

64. G. K. Mukherjee and N. Parihar, *Ann. Geophys.* **22**, 9, 3315-3321, (2004).

65. N. Parihar and G. K. Mukherjee, India, *Adv. Space Res.* **41**, 660-669 (2008).

66. R. Sekar and D. Chakrabarty, *Indian J.of Radio and Space Phys.* **37**, 7, February 2008

67. A. Bhattacharyya and W. J. Burke, *J. Geophys. Res.*, **105**, 24941-24950 (2000)

68. A. Bhattacharyya, *Geophys. Res. Letts.*, **31**, L06806, doi:10.1029/2003GL018960 (2004)

69. A. Bhattacharyya, S. Basu, K. M. Groves, C. E. Valladares and R. Sheehan, *J. Geophys. Res.* **107 (A12)**, 1489, (2002) doi: 10.1029/2002JA009644

70. B. Kakad, K. Jeeva, K. U. Nair and A. Bhattacharyya, *J. Geophys. Res.* **112**, A07311, (2007) doi: 10.1029/2006JA012021

71. C. K. Nayak, D. Tiwari, S. Bose, K. Emperumal and A. Bhattacharyya, RAC (NCRA-TIFR), Udhagamandalam (Ooty), February 26-29, 2008.

72. G. K. Mukherjee: *Terr. Atmos. & Oceanic Sci.* **13(1)**, March (2002).

73. M. Hari Kishore and G. K. Mukherjee, *Curr. Science.* **93(4)**, 488-497 (2007).

74. G. K. Mukherjee, *J. Atmos. Solar -Terr. Phys.* **65**, 379-390 (2003).

75. R. Sridharan, R. Sekar, and S. Gurubaran, *J.Atmos. and Terr. Phys.* **55**, 13, 1661-1663 (1993).

76. R. Sekar, S. Gurubaran, and R. Sridharan, *Ind. J. Radio and Space Phys.* **22**, 197-204, (1993).

77. G. K. Mukherjee, *Earth, Planets Space* (Japan), **58**, 623-632 (2006).

78. G. K. Mukherjee, A. K. Patra and N. Venkateswara Rao, *11th International Workshop on Technical Aspects of MST Radar*, Gadanki, Tirupati, December 11-15 (2006).

79. N. W. Spencer, G. R. Carignan, H. G. Mayr, H. B. Nieman, R. F. Theis, L. E. Wharton and G. R. Carignan, *Geophys. Res. Lett.* **6**, 444-446(1979).

80. G. K. Mukherjee, Navin Parihar, K. Niranjan and G. Manju: *Ind. J. of Radio and Space Phys.* **35**, 14-21, (2006).

81. H. Rishbeth and R. Edwards, *J. Atmos. Terr. Phys.* **51** (4), 321-338 (1989).

82. J. H. Sastri, H.N.R.Rao V.V.Somayajulu and H.Chandra, *Geophys. Res. Lett.* **21**(9), 825-831, (1994).